Dalton Transactions

Accepted Manuscript

ROYAL SOCIETY OF CHEMISTRY

www.rsc.org/dalton

Imatinib Intermediate as a Two in One Dual Channel Sensor for the Recognition of Cu^{2+} and I^- ions in Aqueous Media and its Practical Applications

Samadhan R. Patil[a], Jitendra P. Nandre[a], Devising Jadhav[a], Shilpa Bothra[b], S. K. Sahoo[b], Manisha Devi[c], Chullikkattil P. Pradeep[c], Pramod P. Mahulikar[a]*, Umesh D. Patil[a]*

[a]School of Chemical Sciences, North Maharashtra University, P. B. No.80, Jalgaon - 425 001, (M.S.) INDIA, Tel: +91-0257-2258431; Fax: +91-0257-2258403 E-mail: mahulikarpp@rediffmail.com (PPM), udpatil.nmu@gmail.com (UDP).

[b]Department of Applied Chemistry, S. V. National Institute Technology, Surat-395 007, Gujrat, INDIA.

[c]School of Basic Sciences, Indian Institute of Technology Mandi, Himachal Pradesh, INDIA.

Abstract

A imatinib intermediate 6-methyl-*N*-[4-(pyridin-3-yl)pyrimidin-2-yl]benzene-1,3-diaminepyridopyrimidotoluidine (**PPT-1)** was developed for the colorimetric sensing of Cu^{2+} ions in aqueous solution. With Cu^{2+}, the receptor **PPT-1** showed a highly selective naked-eye detectable color change from colorless to red over the other tested seventy cations. The colorimetric sensing ability of **PPT-1** was successfully utilized in the preparation of test strips and supported silica for the real samples analysis to detect Cu^{2+} ions from 100% aqueous environment. Moreover, the iodide sensing ability of receptor **PPT-1** was explored among the ten examined anions.

Keywords: Chemosensor; Cu^{2+}; Iodide; Colorimetric; Internal charge-transfer.

Introduction

Copper, the third most abundant transition element in humans plays an important role in various physiological processes such as hemoglobin biosynthesis, bone development, dopamine production, and nerve function regulation [1-4]. Similarly, Cu^{2+} ions play critical role as catalytic cofactors for a variety of metallo enzymes such as copper-zinc superoxide dismutase's, lysyloxidase, cytochrome *c* oxidase, and tyrosinase [5-8]. Apart from the biotic significances, copper is extensively used in various industrial, pharmaceuticals and agricultural purposes such as for making alloys, electrical wires, machine parts, batteries and fertilizers etc. [9]. Under normal condition, the average concentration of copper in the blood should not exceeds 100-150 µg/dL, otherwise an increase concentration of copper by any means in the body can cause improper cellular functions and progression of various diseases [10]. Excess accumulation of copper in human because of the widespread utilization leads to serious detrimental effects including neurodegenerative diseases such as Alzheimer's disease, Menkes disease, Wilson's disease, prion disease, amyotrophic sclerosis, lipid metabolism and inflammatory disorders [7-8,11-13]. Therefore, there is a need to develop newer technologies and methods for the qualitative and quantitative detection of copper. In the past literatures, different analytical methods are developed for the detection of Cu^{2+} *viz.* inductively coupled plasma detectors, quantum-dot-based assay, fluorescence anisotropy, surface-plasmon resonance detector, electrochemical and fluorescent sensors, etc [14-15]. These technologies can detect Cu^{2+} ion selectively with high sensitivity but needs highly sophisticated expensive instrumentation. Although fluorescent sensor can have better sensitivity and selectivity with fast response, literature reports tell that the same is not well suited particularly for paramagnetic cations like Cu^{2+} due to their ability to act as fluorescent quencher, which rendered low signal output. Therefore, fluorescent sensors are sometimes less advantageous for the recognition of Cu^{2+} and they give false spectrometric response [16-17]. Alternately,

the absorption based colorimetric chemosensor can be explored because of the distinct visual color change with analyte due to charge transfer band for easy detection by naked-eye.

On the other hand, a considerable research has been focused on the selective recognition of anions in water for monitoring environmental pollution, medicinal diagnostic and the analysis of biological samples [18]. Among thevarious biologically important anions, iodide plays imperative roles in several biological activities such as thyroid gland function and neurological activity. In addition, elemental iodine has been used to synthesize drugs, fine chemicals, and dyes which can be applied in the chemistry, biology and food disciplines [19-20]. Radioactive isotope of iodine is used in medicines and also in analytical chemistry. The iodide content of urine and milk is often required to provide information for nutritional, metabolic and epidemiological studies of thyroid disorder [21-22]. Due to the important roles played by iodide in day to day life, there is also a need for developing simple analytical method to detect iodide in aqueous system. Similar to cations, several methods in literatures are available for iodide detection such as ICP-MS, capillary electrophoresis and iodide-selective electrode [23-24]. Recently, fluorescent sensors have been extensively developed with high sensitivity and selectivity for the detection of iodide [25-28]. However, very few colorimetric chemosensors are available for the detection of iodide in aqueous system [28-30]. Thus, there is a countless demand for the expansion of synthetic receptors capable of selectively recognizing iodide over the other important anions in aqueous system.

Recently, the design and synthesis of imatinib (a derivative of 2-phenylamino-pyrimidine) derivatives has increased immensely due to their anticancer applications. The imatinib is one of the largest selling anticancer drugs and tyrosine kinase inhibitor and used mostly for the treatment of chronic myeloid leukemia and gastrointestinal stromal tumors [31,32]. Imatinib has multistep synthetic pathway and its synthesis goes through a series of intermediates. To date, there was no report on the utilization of imatinib intermediates as a

chemosensor. Also, several chemosensors for recognition of Cu^{2+} or iodide are reported, but very few of them are able to recognize Cu^{2+} and I^- simultaneously in aqueous system (Table S1). Herein, as a part of our ongoing efforts in the field of sensing [33-36] and to address the above stated problems, we have successfully developed an imatinib intermediate (**PPT-1)** for the highly selective and sensitive colorimetric sensing of Cu^{2+} and iodide ions from 100 % aqueous solution. Also, the receptor **PPT-1** was successfully utilized in the development of test strips and supported silica for the detection of Cu^{2+} ions.

Experimental

Materials and Instrumentation

Unless otherwise stated, all the chemicals used for the synthesis of **PPT-1** were of AR grade and were purchased either from S. D. Fine chemicals or Sigma Aldrich depending on their availability. All the solvents were of spectroscopic grade and were used without further treatment. The aqueous stock solutions of cations and anions of concentration 1 x 10^{-2} mol L^{-1} were prepared from their corresponding salt i.e. $AgClO_4$, $Al(ClO_4)_3.9H_2O$, $Ba(ClO_4)_2$, $Ca(NO_3)_2.4H_2O$, $Cd(ClO_4)_2.H_2O$, $Co(ClO_4)_2.6H_2O$, $Cr(ClO_4)_3.6H_2O$, $Fe(ClO_4)_2.xH_2O$, $HgCl_2$, LiBr, $Mg(ClO_4)_2$, $Mn(ClO_4)_2.H_2O$, $Ni(ClO_4)_2.6H_2O$, $Fe(ClO_4)_3.H_2O$, $Pb(ClO_4)_2.3H_2O$, $Zn(ClO_4)_2.6H_2O$, $Cu(ClO_4)_2.6H_2O$, $(n\text{-}Bu)_4NOAc$, $(CH_3\text{-}CH_2\text{-}CH_2\text{-}CH_2)_4NBr$, $(CH_3\text{-}CH_2\text{-}CH_2\text{-}CH_2)_4NCl$, $(CH_3\text{-}CH_2\text{-}CH_2\text{-}CH_2)_4NClO_4$, $(CH_3\text{-}CH_2\text{-}CH_2\text{-}CH_2)_4NCN$, $(n\text{-}Bu)_4NF.xH_2O$, $(CH_3\text{-}CH_2\text{-}CH_2\text{-}CH_2)_4NH_2PO_4$, $(CH_3\text{-}CH_2\text{-}CH_2\text{-}CH_2)_4NHSO_4$, $(CH_3\text{-}CH_2\text{-}CH_2\text{-}CH_2)_4NNO_3$, $(CH_3\text{-}CH_2\text{-}CH_2\text{-}CH_2)_4NI$, respectively. The stock solution of **PPT-1** (1 x 10^{-3} $molL^{-1}$) was prepared by dissolving an accurately weighed **PPT-1** in CH_3CN and then diluted to 3 x 10^{-5} $molL^{-1}$ with CH_3CN:H_2O (40:60) mixed solvent.

The ^1H and ^{13}C-NMR spectra were recorded on an Advance Bruker II 400 MHz Multinuclear probe NMR spectrometer at ambient temperature in $CDCl_3$ with TMS as internal

standard and the chemical shifts were reported in ppm. The electron spray mass spectra were recorded on aQ-TOP micromass (LCMS) mass spectrometer. The IR spectra were recorded on a Perkin Elmer spectrophotometer as KBr discs and the IR bands are expressed in frequency (cm^{-1}). Absorption spectra were recorded on a Perkin Elmer U 3900 Co, USA UV/Visible double beam spectrophotometer. The purity of the compound and progress of the reaction was monitored by means of thin layer chromatography (TLC). Pre-coated silica gel 60 F_{254} (Merck) on alumina plate (7 x 3 cm) were used and visualized by using either iodine or short UV/Visible lamp. Melting points were recorded on the Celsius scale by open capillary method and are uncorrected.

Synthesis of *N*-(5-amino-2-methylphenyl)-4-(3-pyridinyl)-2-pyrimidineamine (PPT-1)

The receptor **PPT-1** was synthesized by adopting the known literature procedure [31 & 37] as shown in Scheme 1. In 100 mL three-necked round bottom flask, equipped with a mechanical stirrer, reflux condenser, and thermometer socket were charged with *N*-(2-methyl-5-nitrophenyl)-4-(pyridin-3-yl)pyrimidin-2-amine (**3**, 0.307 g, 1 mmol) [supporting information], hydrazinemono hydrate (0.154 g of 65% solution in water, 2 mmol), $FeCl_3$ (2.1 mg, 0.013 mmol), active carbon (0.02 g) and water (40 mL). The reaction mass was heated to about 80 ^{0}C for 6-8 hr. Reaction progress was monitored by TLC. After completion of reaction, the reaction mixture was cooled to room temperature. Insoluble materials were filtered off, and the filtrate was extracted with ethyl acetate (10 mL x 5). The combined organic layers was washed with brine and dried over anhydrous Na_2SO_4. The solvent was removed under reduced pressure in vacuo, to get the product as yellow crystals (yield: 80 %); m.p. 140-142 ^{0}C; IR (cm^{-1}) [KBr]: 3360-33050, 2940, 2860, 1633, 1602; Mass [ESI, 70 Ev] *m/z* (%): 279 (26), 278 (65); ^{1}H-NMR (400 MHz, $CDCl_3$, δ ppm): 2.07 (3H, bs, CH_3), 4.87 (2H, s, NH_2), 6.33-6.35 (1H, dd, *J*=4 Hz, ArH), 6.79-6.80 (1H, d, *J*=4 Hz, ArH), 6.86-6.88 (1H, d, *J*=8 Hz, ArH), 7.36-7.38 (1H, d, *J*=12 Hz, ArH), 7.53-7.56 (1H, dd, *J*=4 Hz, ArH),

8.40-8.43 (1H, m, ArH), 8.46-8.48 (1H, d, J=8 Hz, ArH), 8.69-8.71 (2H, m, ArH), 9.25 (1H, s, NH); ^{13}C-NMR (100 MHz, $CDCl_3$, δ ppm): 17.1, 99.8, 103.6, 106.2, 118.3, 121.4, 129.8, 131.2, 134.6, 142.2, 144.3, 146.9, 147.2, 155.6, 160.8, 169.7; Anal. calcd for $C_{16}H_{15}N_5$: C, 69.29; H, 5.45; N, 25.25. Found: C, 69.42; H, 5.43; N, 25.14 (Fig. S1and Fig. S2).

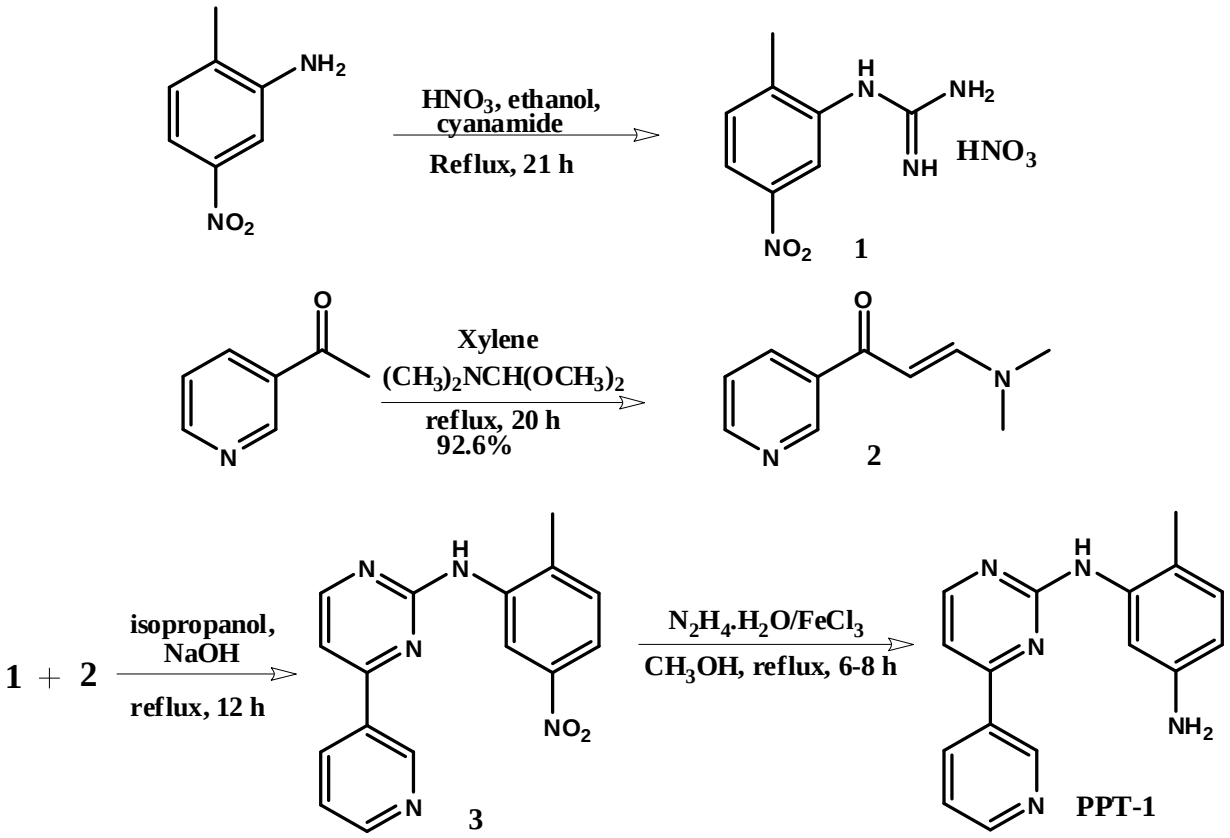

Scheme 1 Synthesis of imatinib intermediate i.e. 6-methyl-*N*1-(4-(pyridin-3-yl)pyrimidin-2-yl)benzene-1,3-diamine (**PPT-1**).

Computational Study

The structural optimization of **PPT-1** and its host-guest complexes with the Cu^{2+} and I^- was performed using the computer program Gaussian 09W [38] by applying the density functional theory (DFT) method. All the DFT calculations were performed in the gas phase with a hybrid functional B3LYP (Becke's three parameter hybrid functional using the LYP correlation functional) using the basis sets 6-31G (d,p) for C, H, N atoms and LANL2DZ for Cu, I atoms.

Results and Discussion

Sensing of Cu^{2+} by PPT-1

The selective and sensitive detection of Cu^{2+} ions in water can be seen from the observed color change of **PPT-1**solution from colorless to dark red (Fig. 1). To perform this naked-eye experiments, 5 equivalents of various cations (30 µL, 1 x 10^{-2} M, in H_2O) including Cu^{2+}ions were added to the solution of **PPT-1** (2 mL, 3 x 10^{-5} M) in CH_3CN:H_2O (40:60, v/v). No significant color change was observed with other cations, which reflects the ability of **PPT-1** to recognize Cu^{2+} ions selectively from aqueous solutions.

Fig. 1 Naked-eye detection of Cu^{2+}ion by **PPT-1**in the presence of other metal cations under visible or sunlight.

The UV-Vis absorption spectra were next recorded to gain more insight into the chemosensing mechanism and binding behavior of **PPT-1** towards different metal cations (Fig. 2). The receptor **PPT-1** exhibited three peaks at 240, 270 and 305 nm in CH_3CN:H_2O (40:60, v/v). The peaks at 240 nm and 270 nm were assigned due to the π→π* electronic transition whereas the maxima at 305 nm was appeared due to the n→σ* or n→π* transition. Upon addition of Cu^{2+} ions (30 µL, 1 x 10^{-2}, in H_2O) to the **PPT-1** solution (2 mL, 3 x 10^{-5} M) in CH_3CN:H_2O (40:60, v/v), two new peaks at 223 nm (a blue-shift of 17 nm from 240 nm) and a broad peak with maxima at 358 nm (a red-shift of 53 nm from 305 nm) were appeared. The spectral shifts accompanied with the color change clearly delineated the formation of a complex species between **PPT-1** and Cu^{2+}. However, other cations (Ag^{+}, Al^{3+}, Ba^{2+}, Ca^{2+}, Cd^{2+}, Co^{2+}, Cr^{3+}, Cu^{2+}, Fe^{2+}, Fe^{3+}, Li^{+}, Mg^{2+}, Mn^{2+}, Ni^{2+}, Pb^{2+}, Zr^{2+}, Zn^{2+} and Hg^{2+}) showed no remarkable changes between the 330 to 400 nm. Further, the competitive experiments

inferred that the selective recognition of Cu^{2+} ions was slightly or not influenced in the presence of various interfering cations in 100 % aqueous medium (Fig. S3).

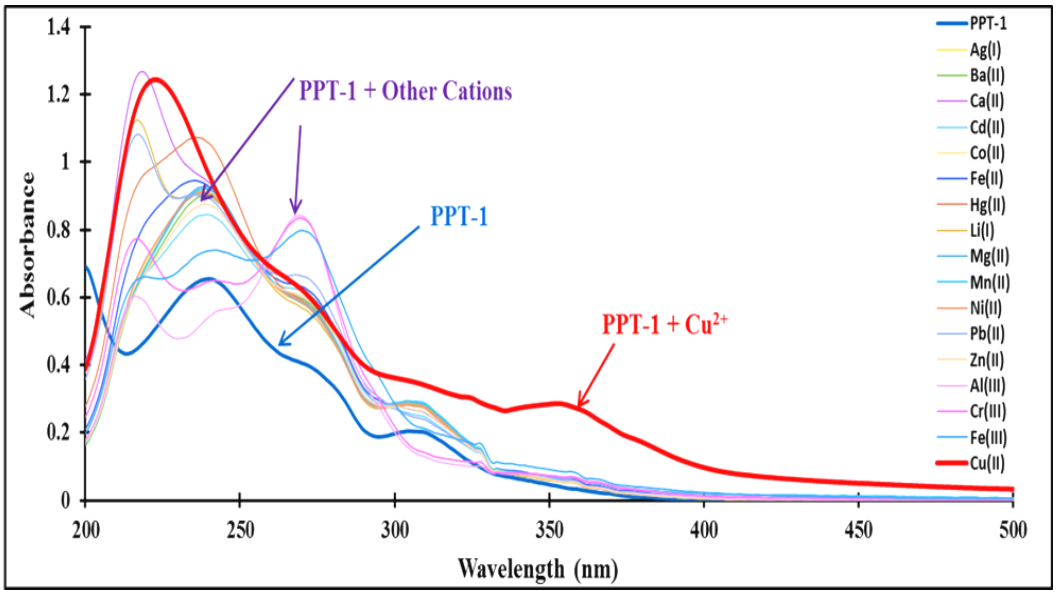

Fig. 2 Absorption spectra of **PPT-1** (3 x 10^{-5} M) in CH_3CN:H_2O (40:60, v/v) upon addition of 5 equivalents of various metal cations (1 x 10^{-2} M, in H_2O).

The UV-Vis absorption titration of **PPT-1** with Cu^{2+} was performed to determine the various analytical parameters such as binding ability, stoichiometry, detection limit etc. The changes in UV-Vis spectrum of **PPT-1** upon successive incremental addition of Cu^{2+} ions is shown in Fig. 3. Upon addition of 1 to 5 equivalents of Cu^{2+} ions to **PPT-1**, the absorbance peaks at 223 nm and 358 nm were increased sharply which may be attributed to the interaction of Cu^{2+} ions with **PPT-1**. Further, to determine the stoichiometry of the formed complex between **PPT-1** and Cu^{2+}, Job's plot (Fig. S4) and mole ratio plot (Fig. S5) methods were employed and the 1:1 stoichiometry was found for the **PPT-1.**Cu^{2+} complex formed in solution. To confirm the mechanism of binding of Cu^{2+} with **PPT-1** we carried out ^{1}H-NMR titrations experiments in which spectra were recorded by adding incremental amounts of copper perchlorate (0, 0.2, 0.5, 1.0 equv.) to the solution of **PPT-1** in $CDCl_3$. Addition of paramagnetic Cu^{2+} affects the NMR resonance frequency of protons which are close to the binding sites of the ligand. It was found that the peak corresponding to $–NH_2$ protons at δ =

3.641 ppm disappears immediately on addition of 0.2 equivalents of Cu^{2+}. Further, additions of Cu^{2+} results in overall broadening of all the peaks of the compound (Fig. S6). The disappearance of peak due to $–NH_2$ proton on addition of 0.2 equivalents of Cu^{2+} confirms the deprotonation and binding of **PPT-1** with copper. The broadening of peaks on addition of more amounts of copper is expected due to the paramagnetic nature of Cu^{2+}. A more direct evidence for the formation of 1:1 complex of **PPT-1** with Cu^{2+} is obtained from the HR-MS analysis of a mixture of **PPT-1** and copper perchlorate in acetonitrile (Fig. S7). A MS peak observed at 414.6850 (calc. = 414.0388) corresponds to [(**PPT-1**-2H+Cu).$2H_2O$+K+H]. Further, the binding or association constant for the complexation of **PPT-1** and Cu^{2+} was obtained from Benesi-Hildebrand plot analysis by using the absorption titration experiments based on 1:1 binding model (Fig.4), and was found to be 5,171 M^{-1}.

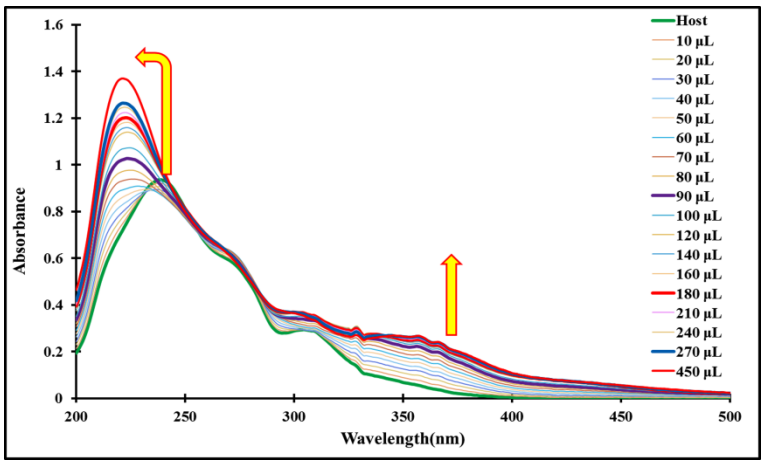

Fig. 3 UV-Vis absorption titration spectra of **PPT-1** (3 x 10^{-5} M) in CH_3CN:H_2O (40:60) with the addition of 1-5 equivalents of Cu^{2+}ions (1 x 10^{-3} M, in H_2O).

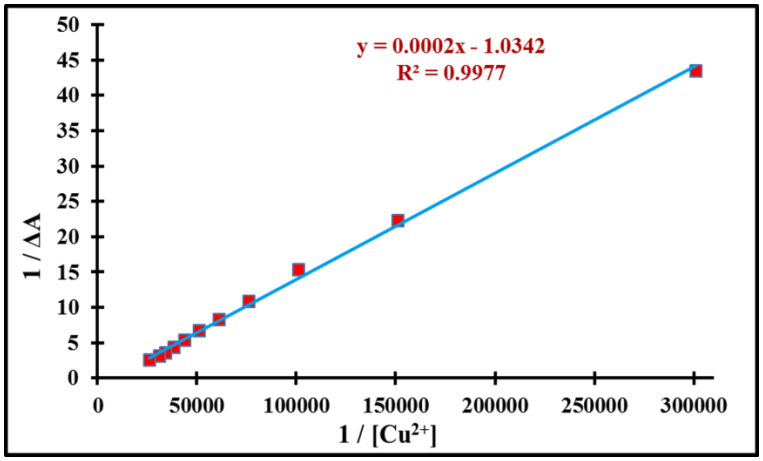

Fig. 4 Benesi-Hildebrand plot of 1/ [A-A_0] against 1 / [Cu^{2+}].

The limit of detection (LOD) and limit of quantification (LOQ) of the receptor **PPT-1** was calculated for Cu^{2+} ions. To calculate the relative standard deviation, the absorption measurements of ten blank samples were taken. The calibration curves (absorbance *vs* [Cu^{2+}]) were plotted (Fig.S8), and then the obtained slope was used to calculate LOD and LOQ values. According to the IUPAC definition, the LOD and LOQ was calculated using the standard relationship i.e. LOD = (3.3 x standard deviation)/slope and LOQ = (10 x standard deviation)/slope. The calculated LOD and LOQ values of **PPT-1** for Cu^{2+} ions are 0.54 µM and 1.6 µM, respectively. This observed LOD and LOQ limits are far superior to the allowed limit of Cu^{2+} for human beings.

Analytical applications of PPT-1

In order to ensure the analytical applicability for the detection of Cu^{2+}, **PPT-1** loaded test strips and silica gelwere prepared. The desired test strips were prepared by soaking small strips of cellulose paper (Whatman) in the solution of **PPT-1** ($1x10^{-2}$ M) in acetonitrile and dried in air. When the strip was dipped in aqueous solution of Cu^{2+} ($1x10^{-3}$ M), the colorless strips sharply turned into dark brown color (Fig. 5 and supporting video). The rapid color change of the test strip in solution clearly inferred the practical application of **PPT-1** for the qualitative detection of Cu^{2+} in aqueous medium.

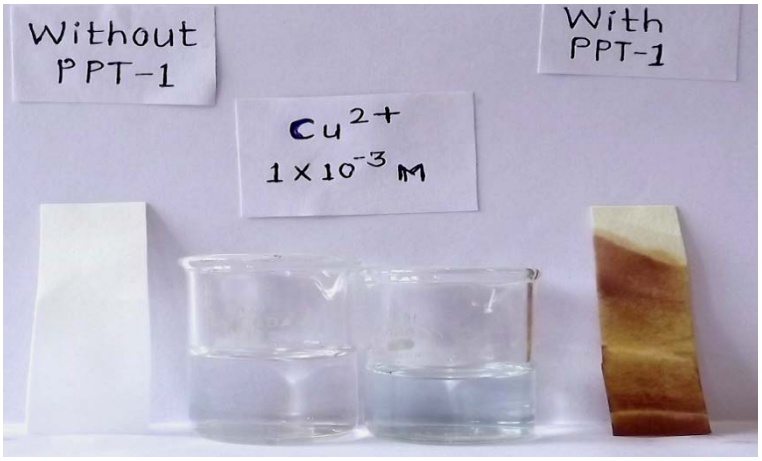

Fig. 5 Practical application of **PPT-1** for detection of Cu^{2+} by test strip method.

Additionally, the qualitive recognition of Cu^{2+} by **PPT-1** was worked on a solid support (Fig. 6 and supporting video). The silica gel (60-120 mesh, 10 g, colorless) was first treated with **PPT-1** (in methanol, 50 mL, $1x10^{-2}$ M) and then dried to get a very very faint yellow color silica gel loaded with the receptor on the surface. When it was treated with 10 mL aqueous solution of Cu^{2+} (A = $1x10^{-3}$ M, B = 1 x 10^{-4} M, D = 1 x 10^{-5} M, E = 1 x 10^{-6} M), the faint yellow color promptly turned to a dark brown color (supporting video). Whereas in bottle 'C' the untreated silica was added into the aqueous solution of Cu^{2+} ions (1 x 10^{-2} M). The prompt color change of the solid silica gel was observed only in the presence of silica loaded with **PPT-1**, which clearly inferred the practical application of **PPT-1** for the qualitative detection of Cu^{2+} in aqueous medium.

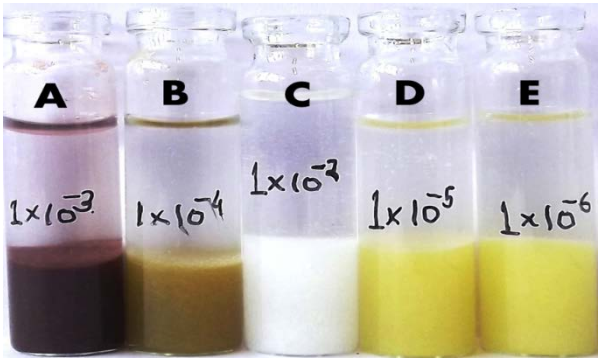

Fig. 6 Practical application of **PPT-1** for detection of Cu^{2+} by silica support method.

Sensing of I^- by PPT-1

The binding profiles of **PPT-1** toward various anions were investigated by UV-Vis absorption spectroscopy. Except I^-, the introduction of various anions of concentration 1 x 10^{-2} M in water did not cause any significant change in the absorption profile of **PPT-1** in $CH_3CN:H_2O$ (40:60, v/v) (Fig. 7). Upon addition of I^- ions to the solution of **PPT-1,** a new intense absorption band at 232 nm was observed. Further, the selective and sensitive detection of I^- in the presence of other competing anions from aqueous solutions was also free from the interference of the other anions (Fig. S8). The above results clearly indicate that the receptor **PPT-1** recognizes I^- selectively over other anions.

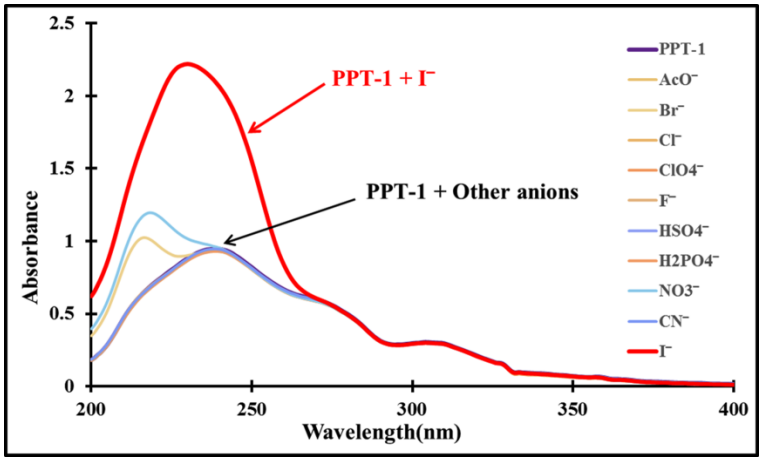

Fig. 7 UV-Vis spectral changes of **PPT-1** (3 x 10^{-5} M) in $CH_3CN:H_2O$ (40:60) upon addition of 5 equivalents of TBA salts of different anions (1 x 10^{-2} M, in H_2O).

The recognition profile and mode of binding of **PPT-1** with I^- was illustrated by performing the absorption titration experiments. Upon continuous addition of I^- (1 x 10^{-3} M, in H_2O) from 1-5 equivalents to the solution of **PPT-1** in $CH_3CN:H_2O$ (40:60, v/v), the intensity of the band at 232 nm was successfully enhanced due to the formation of pseudo cavity of complementary size by **PPT-1** to make electrostatic and/or hydrogen bonding with I^- (Fig. 8). To confirm the mechanism of binding of **PPT-1** with I^-, we carried out ^{1}H-NMR titration experiments in which spectra were recorded by adding varying equivalents of tetrabutylammonium iodide (0, 0.2, 1.0, 4.0, 6.0) to the solution of **PPT-1** in $CDCl_3$. It was

found that the peak corresponding to $-NH_2$ protons at $\delta = 3.641$ ppm undergoes broadening accompanied by a small shift to $\delta = 3.651$ ppm (Fig. S10). The broadening of the peak suggeststhat the I^- sensing is mainly due to hydrogen bonding. To confirm the stoichiometry of binding, we carried out HR-MS studies on acetonitrile solutions of **PPT-1** in presence of I^- anions. Observation of a MS peak at 980.6509 (calc. 980.4284) corresponding to the species [2(**PPT-1**)+I+TBA+K+H_2O], confirms the 2:1 binding stoichiometry (Fig. S11). To get further comprehension concerning the binding stoichiometry, Job's plot and mole ratio plot methods were employed. The Job's plot (Fig.S12) and mole ratio plot (Fig. 8 inset) clearly delineated the formation host-guest complex between **PPT-1** and iodide in 2:1 binding stoichiometry. The association constant or binding constant for the complexation of **PPT-1.**I^- was calculated from Benesi-Hildebrand plot (Fig. 9) and was found to be 5,687 M^{-1}. This high value of binding constant designates the strong binding interactions between **PPT-1** and I^-. In order to check the applicability of receptor **PPT-1**, we have calculated the detection limit and quantification limit for I^- ions. From the straight line regression obtained by the graph plotted between absorbance *vs.* concentration of I^- ions (Fig. S13), the estimated limit of detection (LOD) and limit of quantification (LOQ) for I^- was found to be 0.22 µM and 6.7 µM, respectively.

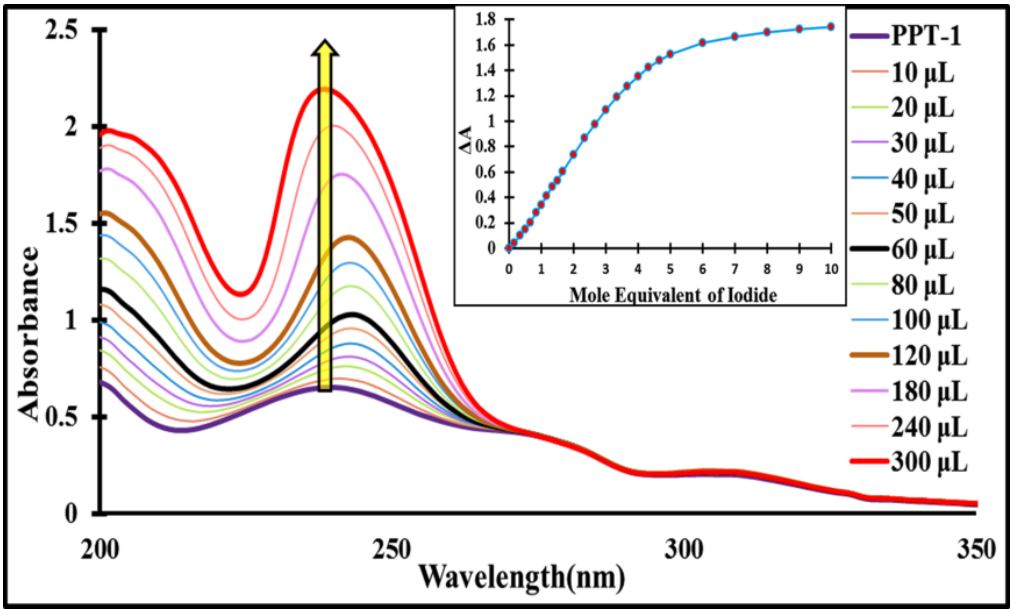

Fig. 8 UV-Vis spectral titration of **PPT-1** (3 x 10^{-5} M) in $CH_3CN:H_2O$ (40:60) upon incremental addition of 1-5 equivalents of iodide (1 x 10^{-3} M, in H_2O).

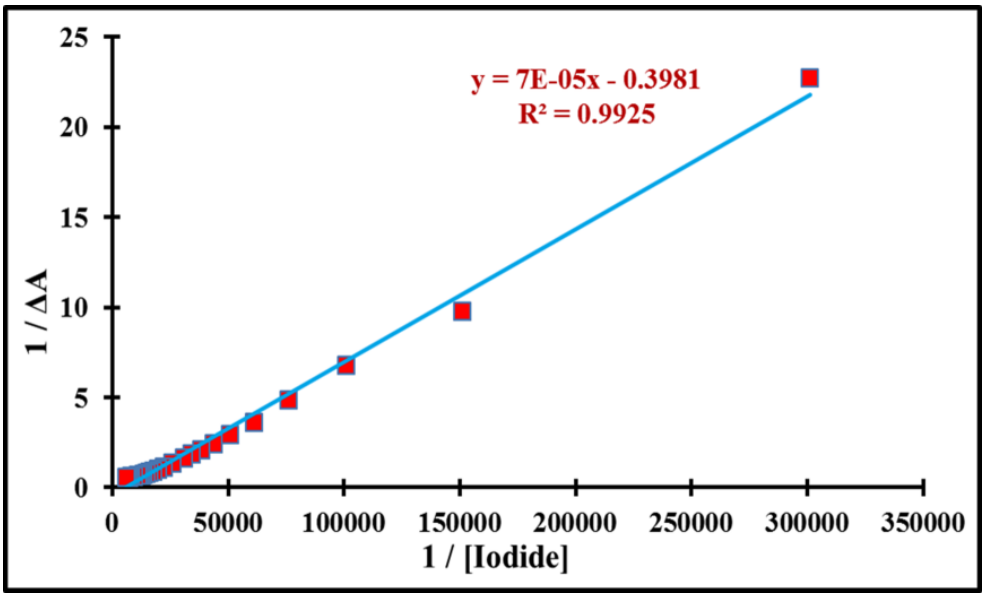

Fig. 9 Benesi-Hildebrand plot of 1/ [A-A_0] against 1/[I$^-$] for binding constant.

Theoreticalresults

The structural optimization of the receptor **PPT-1** and its **PPT-1**.Cu^{2+}/I$^-$ complexes along with the intermolecular charge transfer (ICT) process occurred during the encapsulation of analytes (Cu^{2+} and I$^-$) by **PPT-1** was investigated in the gas phase by applying the exchange-correlation function B3LYP, and the basis sets 6-31G(d,p) (for C, H and N atoms) and LANL2DZ (for Cu and I atoms). The optimized structure of the receptor **PPT-1** and its **PPT-**

1.Cu^{2+}/I^- complexes was shown in Fig. 10. On complexation of **PPT-1** with Cu^{2+} and I^-, the calculated interaction energy ($E_{int} = E_{complex}-E_{receptor}-E_{Cu^{2+}/I^-}$) was lowered respectively by -322.91 kcal/mol and -9.49 kcal/mol which indicates the formation of stable complexes. The receptor **PPT-1** organized itself by a slight molecular twist to encapsulate Cu^{2+} preferably through the pyridine-Nand amine-N atoms. Since the ICT band in **PPT-1** originates from the electron donation from HOMO, localized on the pyrimidine, amino and sp^2-nitrogen substituents to the LUMO, localized on the pyridine ring (Fig. 11), the considerable perturbation in this band on the addition of Cu^{2+} can be ascribed to the stabilization of LUMO and a consequent decrease in the energy gap between HOMO and LUMO. The lowering of energy gap resulted in the observed bathochromic or red-shift of 53 nm in the ICT band and consequently the perceptible change in color from colorless to dark red. On the other hand, the protons at the amine groups ($-NH_2$ and –NH-) can act as both hydrogen bond donor and acceptor, which making an interesting combination for the recognition of iodide anion. The analysis of the molecular electrostatic potential (MEP) map of **PPT-1** (Fig. 10b) also indicates that the two most positive regions shown in blue color are located above the amine protons. On interaction with iodide ion, molecular-twist was observed in the **PPT-1** molecules, which created a pseudo cavity of complementary size to encapsulate iodide ion through multiple weak intermolecular hydrogen bonds. Further, the HOMO and LUMO diagrams of **PPT-1** and $(\mathbf{PPT\text{-}1})_2.I^-$ indicate the internal charge transfer occurred during the iodide recognition between the receptor and iodide ions (Fig. 11).

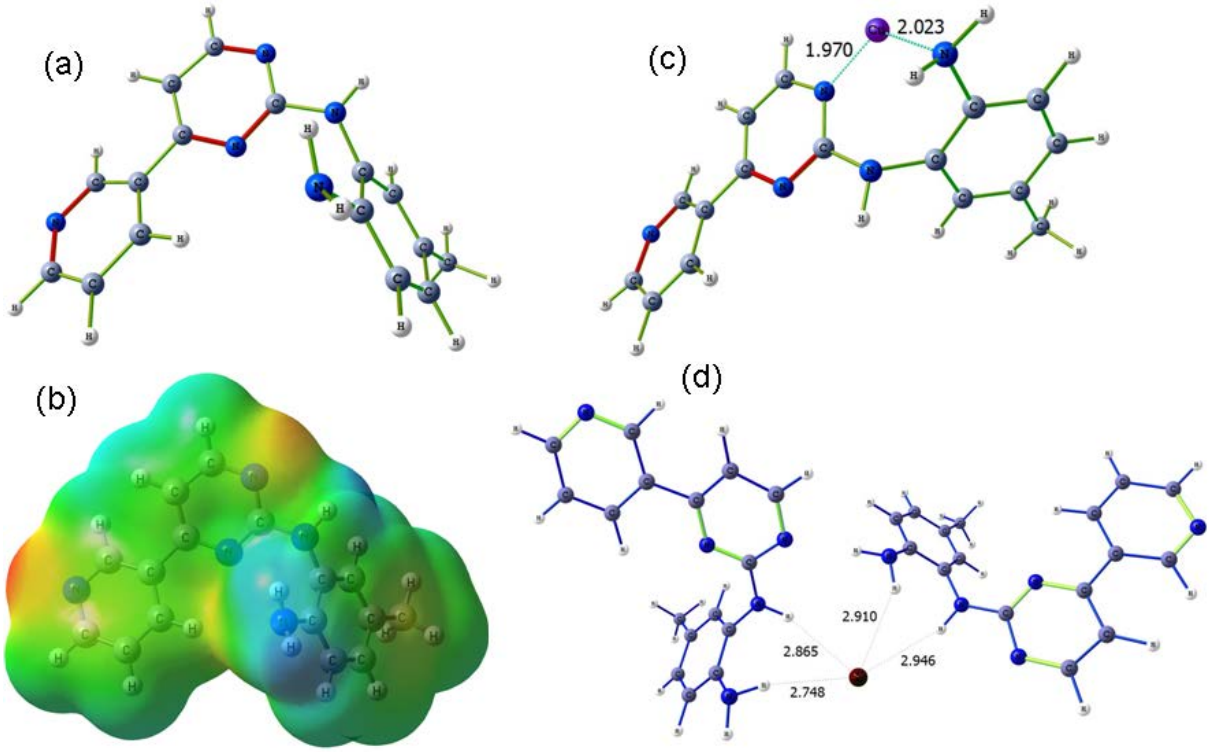

Fig. 10 DFT computed optimized structure of the receptor (a) **PPT-1** withits (b) molecular electrostatic potential (MEP), (c)**PPT-1**.$Cu^{2+}$and (d) **(PPT-1)$_2$.I**in the gas phase.

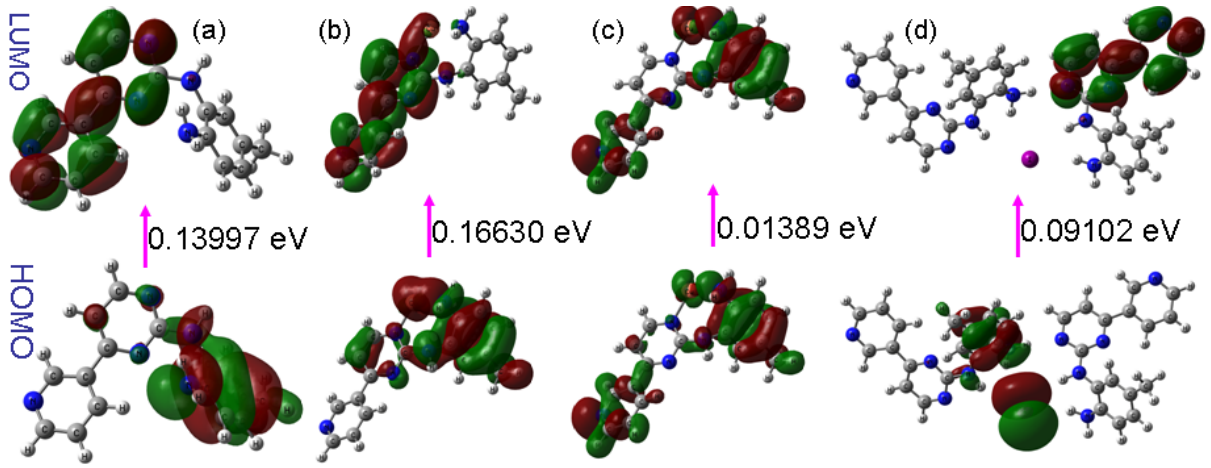

Fig. 11 DFT computed LUMO and HOMO diagrams of (a) receptor **PPT-1**, (c) alpha and (b) beta orbitals of **PPT-1**.Cu^{2+}, and (d) **(PPT-1)$_2$.I** in the gas phase.

Conclusion

In summary, we have successfully developed an imatinib intermediate **PPT-1** as a chemosensor for the recognition of Cu^{2+} and I^- from 100 % aqueous media with high

selectivity and sensitivity. The recognition of Cu^{2+} was confirmed by remarkable color change from colorless to dark red with the appearance of a new charge transfer band. The remarkable colorimetric sensing of **PPT-1** confirmed a 1:1 (**PPT-1**.Cu^{2+}) binding model with the detection limit down to 0.54 µM. Moreover, **PPT-1** can be applied to detect Cu^{2+} in the aqueous media by naked-eye using test strip and silica support methods. Whereas, the iodide ions did not brought any color change of **PPT-1**, but resulted a remarkable spectroscopic response by giving a new intense peak in the absorption spectrum at 232 nm. With **PPT-1**, the iodide ions can be detected up to 0.22 µM in aqueous solution. The good selectivity of chemosensor **PPT-1** for the detection of Cu^{2+} and I^- from pure aqueous medium can opens new doors for many practical applications in chemical, environmental and biological systems.

Acknowledgement

SRP is thankful to DST, New Delhi, India, for financial assistantunder INSPIRE fellowship scheme and Dr. UDP is grateful for the financial support from the DST, New Delhi, India, under FAST TRACK scheme for Young Scientists (Reg. No. CS-088/2013).

Notes and references

1 E. Gaggelli, H. Kozlowski, D. Valensin and G. Valensin, *Chem. Rev.*, 2006, **106**, 1995-2044.

2 E. D. Harris, *J. Trace Elem. Exp. Med.*, 2001, **14**, 207-210.

3 C. Andreini, L. Banci, I. Bertini and A. Rosato, *J. Proteome Res.*, 2008, **7**, 209-216.

4 E. L. Que, D. W. Domaille and C. J. Chang, *Chem. Rev.*, 2008, **108**, 1517-1549.

5 Handbook of metalloproteins, ed. A. Messerschmidt, R. Huber, T. Poulos and K. Weighardt, John Wiley & Sons, Chichester, 2001, vol. 2, pp. 1149-1413.

6 K. D. Karlin, *Science* 1993, **261**, 701-708.

7 B. Halliwell and J. M. C. Gutteridge, *Biochem. J.* 1984, **219**, 1-14.

8 M. C. Linderand M. Hazegh-Azam, *Am. J. Clin.Nutr.,* 1996, **63**, 797S-811S.

9 A. K. Jain, R. K. Singh, S. Jain and J. Raisoni, *Transition Met. Chem.,* 2008, **33**, 243-249.

10 W. T. Tak and S. C. Yoon, *Korean J. Nephrol.,* 2001, **20**, 863-871.

11 K. J. Barnham, C. L. Masters and A. I. Bush, *Nat. Rev. Drug Discov.,* 2004, **3**, 205-214.

12 E. Gaggelli, H. Kozlowski, D. Valensinand G. Valensin, *Chem. Rev.,* 2006, **106**, 1995-2044.

13 E. Madsen and J. D. Gitlin, *Annu. Rev. Neurosci.,* 2007, **30**, 317-337.

14 N. Shao, J. Y. Jin, H. Wang, Y. Zhang, R. H. Yang and W. H. Chan, *Anal. Chem.,* 2008**, 80**, 3466-3475.

15 L. Zhang, L. Shangand and S. Dong, *Electrochem. Commun.,* 2008, **10**, 1452-1454.

16 L. Yang, Q. Song, K. Damit-Og, and H. Cao, Sens. Actuators, B 2013, **176**, 181-185.

17 C. Yu, L. Chen, J. Zhang, J. Li, P. Liu, W. Wang and B. Yan, *Talanta* 2011, **85**, 1627-1633.

18 M. E. Moragues, R. Martinez-Manez and F. Sancenón, *Chem. Soc. Rev.*, 2011, **40**, 2593-2643.

19 M. Vetrichelvan, R. Nagarajan and S. Valiyaveettil, *Macromolecules* 2006, **39**, 8303-8310.

20 H. Kim and J. Kang, *Tetrahedron Lett.*, 2005, **46**, 5443-5445.

21 M. Haldimann, B. Zimmerli, C. Als and H. Gerber, *Clin. Chem.,* 1998, **44**, 817-824, and references therein.

22 F. Jalali, M. J. Rajabi, G. Bahrami and M. Shamsipur, *Anal. Sci.*, 2005, **21**, 1533-1537.

23 S. Chandra, K. S. Lokesh, H. Lang, Sens. Actuators, B 2009, **137**, 350-356.

24 K. Ito, T. Ichihara, H. Zhuo, K. Kumamoto, A. R. Timerbaev and T. Hirokawa, *Anal. Chim. Acta*, 2003, **497**, 67-74.

25 N. Singh, H. J. Jung and D. O. Jang, *Tetrahedron Lett.*, 2009, **50**, 71-74.

26 K. Ghosh and T. Sen, *Tetrahedron Lett.*, 2008, **49**, 7204-7208.

27 K. R. Rathikrishnan, V. K. Indirapriyadharshini, S. Ramakrishna and R. Murugan, *Tetrahedron* 2011, **67**, 4025-4030.

28 Y. Zhao, L. Yao, M. Zhang and Y. Ma, *Talanta* 2012, **97**, 343-348.

29 K. Ghosh and I. Saha, *Supramol. Chem.*, 2010, **22**, 311-317.

30 J.-H. Choi, I.-H.Ahn, J. L. Sessler and D.-G. Cho, *Supramol. Chem.*, 2011, **23**, 283-286.

31 Y.-F. Liu, C.-L. Wang, Y.-J. Bai, N. Han, J.-P. Jiao and X.-L. Qi, *Org. Process Res. Dev.*, 2008, **12**, 490-495.

32 H. Liu, W. Xia, Y. Luo and W. Lu, *Monatsh Chem.*, 2010, **141**, 907-911.

33 J. Nandre, S. Patil, V. Patil, F. Yu, L. Chen, S. Sahoo, T. Prior, C. Redshawd, P. Mahulikar and U. Patil, Biosens. Bioelectronics 2014, 61, 612-617.

34 A. S. Kuwar, U. A. Fegade, K. C. Tayade, U. D. Patil, H. Puschmann, V. V. Gite, D. S. Dalal and R. S. Bendre, *J. Fluoresc.*, 2013. **23**, 859-864.

35 S. K. Sahoo, D. Sharma, R. K. Bera, G. Crisponi and J. F. Callan, *Chem. Soc. Rev.*, 2012, **41**, 7195-7227.

36 A. K. Gupta, A. Dhir and C. P. Pradeep, Dalton Trans., 2013, **42**, 12819-12823.

37 K. A. Kalesh, D. S. B. Sim, J. Wang, K. Liu, Q. Lin and S. Q. Yao, *Chem. Commun.*, 2010, **46**, 1118-1120.

38 H. B. Schlegel, G. E. Scuseria, M. A. Robb, J. R. Cheeseman, G. Scalmani, V. Barone, B. Mennucci, G. A. Petersson, H. Nakatsuji, M. Caricato, X. Li, H. P. Hratchian, A. F. Izmaylov, J. Bloino, G. Zheng, J. L. Sonnenberg, M. Hada, M. Ehara, K. Toyota, R. Fukuda, J. Hasegawa, M. Ishida, T. Nakajima, Y. Honda, O. Kitao, H. Nakai, T. Vreven, J. A. Montgomery, Jr., J. E. Peralta, F. Ogliaro, M. Bearpark, J. J. Heyd, E. Brothers, K. N. Kudin, V. N. Staroverov, R. Kobayashi, J. Normand, K. Raghavachari, A. Rendell, J.

C. Burant, S. S. Iyengar, J. Tomasi, M. Cossi, N. Rega, J. M. Millam, M. Klene, J. E. Knox, J. B. Cross, V. Bakken, C. Adamo, J. Jaramillo, R. Gomperts, R. E. Stratmann, O. Yazyev, A. J. Austin, R. Cammi, C. Pomelli, J. W. Ochterski, R. L. Martin, K. Morokuma, V. G. Zakrzewski, G. A. Voth, P. Salvador, J. J. Dannenberg, S. Dapprich, A. D. Daniels, Ö. Farkas, J. B. Foresman, J. V. Ortiz, J. Cioslowskiand D. J. Fox, Gaussian 09, Revision A.1, Gaussian, Inc., Wallingford CT(2009).

39 P. Kaur, S. Kaur, K. Singh, P. R. Sharma and T. Kaur, Dalton Trans., 2011, **40**, 10818-10821.

40 S. Sirilaksanapong, M. Sukwattanasinitt and P. Rashatasakhon, Chem. Commu., 2012, **48**, 293-295.

Graphical Abstract